HHS Public Access

Author manuscript

Magn Reson Med. Author manuscript; available in PMC 2022 March 01.

Published in final edited form as:

Magn Reson Med. 2021 March ; 85(3): 1175–1182. doi:10.1002/mrm.28489.

Assessment of hepatic pyruvate carboxylase activity using hyperpolarized [1-^{13}C]-L-lactate

Jun Chen[1], **Edward P. Hackett**[1], **Zoltan Kovacs**[1], **Craig R. Malloy**[1,2,3], **Jae Mo Park**[1,3,4]

[1.]Advanced Imaging Research Center, The University of Texas Southwestern Medical Center, Dallas TX USA 75390

[2.]Department of Internal Medicine, The University of Texas Southwestern Medical Center, Dallas TX USA 75390

[3.]Department of Radiology, The University of Texas Southwestern Medical Center, Dallas TX USA 75390

[4.]Department of Electrical and Computer Engineering, The University of Texas at Dallas, Richardson TX USA 75080

Abstract

Purpose: To evaluate the utility of hyperpolarized [1-^{13}C]-L-lactate to detect hepatic pyruvate carboxylase (PC) activity *in vivo* under fed and fasted conditions.

Methods: [1-^{13}C]-labeled sodium L-lactate was polarized using a SPINlab polarizer. Polarization level and the T_1 were measured *in vitro* in a 3T MR scanner. Two groups of healthy rats (fasted *vs.* fed) were prepared for *in vivo* studies. Each rat was anesthetized and intravenously injected with 60-mM hyperpolarized [1-^{13}C]-L-lactate, immediately followed by dynamic acquisition of ^{13}C MR spectra from the liver at 3T. The dosage-dependence of the ^{13}C-products was also investigated by performing another injection of an equal volume of 30-mM hyperpolarized [1-^{13}C]-L-lactate.

Results: T_1 and liquid polarization level of [1-^{13}C]-L-lactate were estimated as 67.8 sec and 40.0%, respectively. Besides [1-^{13}C]pyruvate and [1-^{13}C]alanine, [^{13}C]HCO_3^- and [1-^{13}C]aspartate were produced from hyperpolarized [1-^{13}C]-L-lactate in rat liver. Smaller HCO_3^- and larger aspartate were measured in the fed group compared to the fasted group. Pyruvate and alanine production were increased in proportion to the lactate concentration, whereas the amount of HCO_3^- and aspartate production was consistent between 30-mM and 60-mM lactate injections.

Conclusion: This study demonstrates that a unique biomarker of PC flux, the appearance of [1-^{13}C]aspartate from [1-^{13}C]-L-lactate, is sensitive to nutritional state and may be monitored *in vivo* at 3T. Since [^{13}C]HCO_3^- is largely produced by PDH flux, these results suggest that the ratio of [1-^{13}C]aspartate and [^{13}C]HCO_3^- (aspartate/HCO_3^-) reflects the saturable PC/PDH enzyme activities.

Correspondence to: Jae Mo Park, Ph.D., The University of Texas Southwestern Medical Center, 5323 Harry Hines Blvd. Dallas TX 75019, jaemo.park@utsouthwestern.edu, +1-214-645-7206.

Keywords

Hyperpolarized ^{13}C; lactate; pyruvate carboxylase; pyruvate dehydrogenase; liver; aspartate; bicarbonate

Introduction

Pyruvate can be metabolized in mitochondria either by pyruvate carboxylase (PC) or the pyruvate dehydrogenase (PDH) complex. PC catalyzes the carboxylation of pyruvate to oxaloacetate (OAA) for biosynthesis whereas PDH decarboxylates pyruvate to generate acetyl-CoA, CO_2, and energy(1). PC plays a critical role in hepatic anaplerosis, the process for replenishing tricarboxylic acid (TCA) cycle intermediates(2). Understanding and measuring the balance between pyruvate carboxylation and decarboxylation in intact liver is a long-standing challenge because both pathways involve the TCA cycle. Moreover, the role of pyruvate carboxylation is often enhanced in liver diseases such as in non-alcoholic fatty liver disease and type 2 diabetes due to the increased gluconeogenesis(3).

Dynamic nuclear polarization (DNP) of [1-^{13}C]pyruvate allows real-time observation of cellular metabolism and *in vivo* enzyme activities by detecting metabolic products such as lactate, alanine, and HCO_3^- (bicarbonate)(4, 5). However, in some respects hyperpolarized [1-^{13}C]pyruvate is not ideal for studies of hepatic metabolism. For example, HCO_3^- can be produced from both PDH and PC pathways (Fig.1), and previous studies illustrated the difficulties of interpreting HCO_3^- production from hyperpolarized [1-^{13}C]pyruvate as PC activity(6–8). Detection of additional products in either pathway can clarify the fractional contribution of the pathways to the [^{13}C]HCO_3^- production. Further, studies with hyperpolarized [1-^{13}C]pyruvate are inevitably associated with hyperpolarized [1-^{13}C]pyruvate hydrate. Unfortunately, the hydrate C1 resonance frequency at 179.8 ppm is in the middle of a metabolically relevant region of the spectrum occupied by malate C1, malate C4 aspartate C1, aspartate C4, and fumarate C1/C4, ranging from about 175 to 181 ppm. These are the products of carboxylation of [1-^{13}C]pyruvate and are readily detectable in the liver at higher fields where chemical shift dispersion is sufficient. Indeed, Lee, *et al.* measured hepatic pyruvate carboxylation by detecting aspartate, malate, and fumarate from hyperpolarized [1-^{13}C]pyruvate at 9.4T(9). However, the PC-specific products are difficult to resolve at 3T and often dominated by the large pyruvate and pyruvate hydrate peaks. A third issue is that a bolus of pyruvate may itself disrupt the balance between PDH and PC fluxes. As the components of the lactate dehydrogenase (LDH) reaction are always in equilibrium *in vivo* an increase in the concentration of pyruvate in the cytosol will alter the tissue NAD^+/NADH ratio although the impact of changes in extracellular lactate or pyruvate will depend on transport, activity of LDH, and other factors(10–12). As a result, the increased cytosolic NAD^+/NADH ratio shunts pyruvate through PDH and away from carboxylation due to both mass action and a change in redox (Fig.2A). Within minutes this effect is overcome and pyruvate can enter the TCA cycle via PC, but by this time much of the polarization is lost. Since plasma and tissue [lactate] are typically 10-fold greater than pyruvate, injecting an equimolar bolus of hyperpolarized lactate will have much less effect on redox and should be preferable for detecting PC activity (Fig.2B).

Lactate is the key metabolite of the Cori cycle and also the major substrate for liver gluconeogenesis(13). The control strength of PC for lactate gluconeogenesis is much greater for PC than for other enzymes of the pathway, making lactate a good probe to study PC activity in the liver(14). Hyperpolarized [1-^{13}C]-L-lactate has also been shown to be effective for *in vivo* metabolic studies(15–19). [1-^{13}C]-L-lactate can lead to the production of [1-^{13}C]pyruvate, which would be converted by PC into [1-^{13}C] or [4-^{13}C]OAA (after backwards scrambling into the symmetric intermediates, fumarate and succinate) and subsequently into [1-^{13}C] or [4-^{13}C]aspartate (Fig.1). Further metabolism of [1-^{13}C] or [4-^{13}C]OAA will yield ^{13}C-labeled HCO_3^-, citrate or [1-^{13}C]pyruvate, depending on the balance between citrate synthase and phosphoenolpyruvate carboxykinase (PEPCK). Moreover, due to the tightly regulated pyruvate pool size, we expect to have smaller pyruvate and pyruvate hydrate peaks from hyperpolarized [1-^{13}C]-L-lactate, permitting resolution of the aspartate, malate, and fumarate resonances. Therefore, we hypothesized that hyperpolarized L-lactate is a more suitable substrate than pyruvate to investigate PC activity in the liver at 3T. In this study, we assessed hepatic metabolism in fed and overnight fasted rats using hyperpolarized [1-^{13}C]-L-lactate to demonstrate the feasibility of measuring PC/PDH balance *in vivo*. We further investigated dosage-dependence of metabolic profiles by comparing the products from 60-mM and 30-mM hyperpolarized [1-^{13}C]-L-lactate.

Methods

Substrates and polarization procedure

Sodium [1-^{13}C]-L-lactate was purchased from Cambridge Isotope Laboratories, Inc. (Tewksbury MA, USA). 2.1-M [1-^{13}C]-L-lactate was prepared in 4:1 w/w water:glycerol with 15-mM OX063 as previously described(15, 16). A SPINlab™ polarizer (GE Healthcare, Waukesha WI, USA) that operates at 5T and ~0.8 K was used for polarizing [1-^{13}C]-L-lactate. 90 or 180 μL of the lactate sample was placed in a sample vial and assembled with a research fluid path (GE Healthcare), which included 16 mL of dissolution media containing 0.1 g/L of disodium ethylenediaminetetraacetate (Na_2EDTA). The sample was dissolved after approximately 5 hours of polarization, yielding ~6.0 mL of 30- or 60-mM hyperpolarized [1-^{13}C]-L-lactate. Liquid polarization level and longitudinal relaxation time (T_1) of hyperpolarized [1-^{13}C]-L-lactate were calculated from independent *in vitro* measurements as described in the Supporting Information.

Animal preparation and MR protocols

All the *in vivo* MR studies were performed using a clinical 3T MR scanner (GE Discovery 750w). Two groups of healthy male Wistar rats (n=10, 291–517g) were used in the study. One group was fasted overnight (>14 hours, n=6) before the examination. The second group was examined in the fed state (n=5). One rat was measured at both conditions. Rat were anesthetized with 2–3% isoflurane in oxygen (~1.5L/min). A custom-built ^{13}C radiofrequency (RF) surface coil (diameter Ø = 28mm) was placed on top of the liver area for both RF excitation and data acquisition. After shimming over the liver region using a ^{1}H point-resolved spectroscopy (PRESS) sequence, a baseline ^{13}C NMR free induction decay (FID) signal was acquired prior to injecting hyperpolarized material. Subsequently, each rat

was injected via tail vein with 60-mM hyperpolarized [1-^{13}C]-L-lactate (0.75mmol/kg body weight, up to 4.0mL, injection rate = 0.25mL/s), immediately followed by a non-localized dynamic pulse-and-acquire spectroscopy sequence (TR = 3sec, 32-μsec 10° hard pulse, scan time = 4min, spectral width = 5,000Hz, spectral points = 2,048). The RF transmit gain was pre-calibrated for 90° excitation using a gadolinium-doped 1-M [^{13}C]bicarbonate ball phantom (Ø = 30mm) and adjusted for the 10° nominal flip angle (flip angle ranges 8–14° for <1.5 cm distance). A subset of the animals (n=3 for each group) underwent a second scan with additional injection of 30-mM hyperpolarized [1-^{13}C]-L-lactate (0.375mmol/kg body weight). To ensure the second injection is not affected by the initial injection, we waited for 30min from the first injection for the rat to clear the labeled lactate before next injection. Animal vital signs were monitored throughout the session and the respiratory rate was maintained at 40–60 breaths/min by adjusting the isoflurane level. All the procedures were approved by the local Institutional Animal Care and Use Committee.

Data reconstruction and kinetic analysis

All the ^{13}C data were reconstructed using MATLAB (Mathworks, Natick MA, USA). FID data at each time point was apodized with a 5-Hz Gaussian filter, zero-filled 4-fold, and Fourier transformed. As needed, the FID data were subtracted from the baseline FID, described above, to remove a natural abundance lipid peak at 172.7 ppm, which partially overlaps the [1-^{13}C]pyruvate resonance. Three analytical methods were used to quantitatively assess [^{13}C]HCO_3^- and [1-^{13}C]aspartate, produced from hyperpolarized [1-^{13}C]-L-lactate. First, area under the curve (AUC) of each metabolite's time curve was calculated by integrating the corresponding peak from the dynamically summed spectrum in absorption mode after 0th and 1st order phase corrections. Second, the AUCs were normalized by the total carbon signal (tC = lactate_{AUC} + pyruvate_{AUC} + alanine_{AUC} + $HCO_3^-{}_{AUC}$ + aspartate_{AUC}) and metabolite ratios (aspartate/HCO_3^-). Lastly, apparent conversion rate constants (*k*'s) were calculated by fitting the peak-integrated time curves of lactate and the products using the multi-site exchange model that is described in the Supporting Information. All the data were presented as mean ± standard error. Statistical significance between fasted and fed groups was tested using non-paired Student's *t-test* (α=0.05, two-tailed analysis). Paired *t-test* (α=0.05, two-tailed analysis) was used for comparing 30-mM and 60-mM lactate results.

Results

Polarization level of [1-^{13}C]-L-lactate was 40.0 ± 0.53% (n=3) at the time of dissolution. The *in vitro* T_1 was measured as 67.8 ± 0.56 sec.

Time-averaged ^{13}C spectra acquired after an injection of 60-mM hyperpolarized [1-^{13}C]-L-lactate in a fasted and fed rat liver *in vivo* are shown in Figure 3. [1-^{13}C]Lactate (183.5 ppm), [1-^{13}C]pyruvate (171.3 ppm), [1-^{13}C]alanine (177.0 ppm), [1-^{13}C]aspartate (175.5 ppm) peaks were detected from all the fasted rats ($\text{aspartate}_{AUC} = 4.3 \pm 0.9 \times 10^5$, aspartate/tC = 0.0047 ± 0.0011, n = 5) while [^{13}C]HCO_3^- peak at 161.9 ppm was just above the noise level ($HCO_3^-{}_{AUC} = 1.0 \pm 0.4 \times 10^5$, HCO_3^-/tC = 0.0011 ± 0.0005), suggesting higher PC activity and lower PDH activity in the fasted animals (Fig.3A) compared to the

fed animals (Fig.3B). Other PC-specific metabolites such as malate, fumarate, or [4-^{13}C]aspartate were not resolved due to the adjacent alanine and pyruvate peaks. The fed rats produced significantly more [^{13}C]HCO_3^- ($HCO_3^-{}_{AUC}$ = 15.7 ± 4.5 × 10^5, HCO_3^-/tC = 0.0117 ± 0.0010, P < 0.002) and less [1-^{13}C]aspartate (aspartate$_{AUC}$ = 0.52 ± 0.15 × 10^5, aspartate/tC = 0.0005 ± 0.0001, P = 0.006). Aspartate-to-HCO_3^- ratio was significantly lower in fed condition (0.069 ± 0.039) than fasted condition (2.65 ± 0.77, P = 0.01). AUCs of the metabolite peaks normalized to tC are summarized in the Supporting Information Table S1.

The dynamic changes of metabolites in rat livers after a bolus injection of 60-mM hyperpolarized [1-^{13}C]lactate in fasted and fed states are illustrated in Figure 4, including experimental data (lines) and results of fitting (symbols). The apparent lactate conversion rate constants ($k_{Lac\rightarrow Pyr}$) was not statistically significant (P = 0.09) between the fasted rats (0.0075 ± 0.0008 sec^{-1}) and the fed rats (0.0099 ± 0.0009 sec^{-1}). Pyruvate to alanine conversion ($k_{Pyr\rightarrow Ala}$) was calculated as 0.45 ± 0.04 sec^{-1} for fasted and 0.48 ± 0.05 sec^{-1} for fed conditions (P = 0.7). Pyruvate to HCO_3^- conversion ($k_{Pyr\rightarrow Bic}$) was significantly larger in the fed group (0.18 ± 0.03 sec^{-1}) than the fasted group (0.0034 ± 0.0017 sec^{-1}, P < 0.001). Conversely, pyruvate to aspartate conversion rate constant ($k_{Pyr\rightarrow Asp}$) was significantly smaller in the fed group (0.0013 ± 0.0002) than the fasted group (0.065 ± 0.007 sec^{-1}, P < 0.0001). Kinetic data are summarized in the Supporting Information Table S2.

Figure 5 compares the time-averaged ^{13}C spectra acquired after an injection of 60-mM (red) and 30-mM (blue) hyperpolarized [1-^{13}C]-L-lactate from the same rat. For the fed liver, pyruvate and alanine production were approximately proportional to the lactate concentration, resulting comparable pyruvate$_{AUC}$/tC (P = 0.33) and alanine$_{AUC}$/tC (P = 0.89) between the two injections. The amount of HCO_3^- production was independent of the concentration of injected hyperpolarized lactate, and thus, the normalized HCO_3^- was significantly smaller with higher lactate concentration (HCO_3^-/tC = 0.012 ± 0.002 for 60-mM, 0.026 ± 0.003 for 30-mM, P = 0.05). Similar result was observed in fasted condition; pyruvate and alanine production were still proportional to the lactate concentration with comparable pyruvate$_{AUC}$/tC (P = 0.82) and alanine$_{AUC}$/tC (P = 0.11) between two injections while [1-^{13}C]aspartate production was unchanged and normalized aspartate significantly increased (P < 0.05).

Discussion

Similar to pyruvic acid, neat lactic acid polarizes well without a glassing agent. Like pyruvic acid (14M), the high concentration of lactic acid (13.4M) enables a small sample volume, facilitating rapid dissolution of a large amount of hyperpolarized lactate solution. All factors favor *in vivo* studies. However, assessment of the PC-related metabolites from lactic acid is hampered by the acid-catalyzed formation of polymers(20). The dimeric lactate generates two large peaks that overlap with [1-^{13}C]alanine and [1-^{13}C]pyruvate hydrate, and interfere with assessing PC-related metabolites. To avoid the polymers, we chose sodium lactate. The longitudinal relaxation time of [1-^{13}C]-L-lactate and the polarization level were almost comparable to those of [1-^{13}C]pyruvate due to the similarity in molecular structure. The higher liquid polarization level (40.0%), as compared to that reported in the previous

literatures (25.3%, 27.8%)(15, 16), is primarily due to the improved hardware performance such as stronger magnetic field and a lower operating temperature. The longer T_1 (67.8 sec), as compared to the previous studies (39.0 sec, 41.2 sec)(15, 16), was probably due to the absence of gadolinium in the lactate sample. When the lactate sample was mixed with a gadolinium complex (1-mM Magnevist in the DNP sample, ~20 μM after dissolution), the T_1 was found to be 44.8 seconds as demonstrated in the Supporting Information Figure S2. Indeed, the ^{13}C T_1 shortening effect of Gd-complexes is already reported in the literature. The longitudinal ^{13}C relaxivity of Onmiscan, a gadolinium complex that is similar to Magnevist, towards ^{13}C-labeled glutamate was found to be 0.5 mM^{-1} sec^{-1} and this study concluded that the presence of a Gd-agent with a ^{13}C relaxivity of 0.5 mM^{-1} sec^{-1} should be detectable at 20μM(21).

In this study, we assessed metabolic products from hyperpolarized L-lactate in the liver under fed and fasted conditions. Two different nutritional states were chosen because hepatic PDH and PC activities are tightly regulated in response to diet. PDH is highly active when an animal is well fed and is gradually shut down by phosphorylation during starvation(22). On the other hand, PC activity increases significantly during a fast(23). Consistent with these earlier conclusions, we found that fasted liver was associated with baseline-level [^{13}C]HCO_3^- peak, whereas the [^{13}C]HCO_3^- peak is prominent in fed liver (Fig.3). However, the appearance of [^{13}C]HCO_3^- alone does not distinguish pyruvate carboxylation from decarboxylation (Fig.1). Unlike [^{13}C]HCO_3^-, the appearance of hyperpolarized [1-^{13}C]aspartate from hyperpolarized [1-^{13}C]-L-lactate is exclusively due to carboxylation of pyruvate under these conditions. As demonstrated in previous hyperpolarization studies, direct detection of PC product at 3T is difficult. For instance, although hyperpolarized [2-^{13}C]pyruvate is feasible to detect PC flux, a previous study reported production of PC-specific [3-^{13}C]citrate at just above the noise level in a time-averaged spectrum(24). This [1-^{13}C]aspartate peak, on the other hand, was reliable enough to allow kinetic analysis in all the fasted rats. The significantly reduced pyruvate and alanine peaks produced from hyperpolarized lactate as compared to those from hyperpolarized pyruvate injection are favorable to [1-^{13}C]aspartate detection. For instance, previous rodent studies using hyperpolarized [1-^{13}C]pyruvate could not detect any [1-^{13}C]aspartate in the liver under both fed and fasted conditions(8, 25). Since both [^{13}C]HCO_3^- and [1-^{13}C]aspartate could be monitored simultaneously from hyperpolarized lactate, these results indicate that PC activity may be monitored *in vivo* and this activity is sensitive to nutritional state. Furthermore, increased hyperpolarized [^{13}C]HCO_3^- signal in absence of aspartate peak under fed condition indicate that much or all of [^{13}C]HCO_3^- is derived from PDH-mediated decarboxylation (Fig.1)(6, 8).

Metabolized [1-^{13}C]OAA from PC activity would go through label scrambling in the TCA cycle to form [4-^{13}C]OAA and subsequently [1-^{13}C]aspartate and [4-^{13}C]aspartate (Fig.1). [4-^{13}C]Aspartate peak at 178 ppm, which overlaps with the pyruvate hydrate peak, and therefore, was not detectable in the study. Thus, [1-^{13}C]aspartate, which is approximately a half of the total labeled aspartate, was the best estimate for the PC activity. The absence of [4-^{13}C]aspartate peak in the spectra could be due to polarization loss by the additional metabolic reactions. Unlike [1-^{13}C]aspartate, which is generated directly from oxaloacetate, production of [4-^{13}C]aspartate requires backward scrambling of oxaloacetate to fumarate

and malate in the TCA cycle. This requires additional binding to enzymes, which can accelerate loss of hyperpolarized ^{13}C signals, making [4-^{13}C]aspartate more difficult to detect than [1-^{13}C]aspartate(26).

In fasted animals, the amount of [1-^{13}C]aspartate production remained the same after a bolus of 30-mM [1-^{13}C]lactate compared to an equal volume of 60-mM lactate (Fig.5A), suggesting that the hepatic PC flux was saturated after injection of 30-mM lactate bolus. Likewise, no significant difference in production of [^{13}C]HCO_3^- between the two different lactate concentration in fed liver (Fig.5B), indicating saturation of PDH. Therefore, [1-^{13}C]aspartate and [^{13}C]HCO_3^- should be carefully quantified to properly describe the activity of both enzymes. Peak integration from the time curves (AUC) is ideal as it gives the absolute quantification of the product. However, it is not practical, considering the inter-subject variability (e.g., liver mass, coil positioning) and the injection parameters (e.g., variability in solid-state polarization, dissolution volume, dissolution-to-injection time, dosage). Normalization with the lactate peak or total carbon (tC) signals are independent of the problems associated with the AUCs, but do not reflect the saturable PC/PDH activities. Similarly, apparent conversion rate constants (k's) from kinetic analysis are not appropriate for PC and PDH conversions ($k_{Pyr\rightarrow Asp}$, $k_{Pyr\rightarrow Bic}$) when the amount of locally delivered substrate is unknown as they are heavily relying on the substrate concentrations. Therefore, we suggest that [1-^{13}C]aspartate-to-[^{13}C]HCO_3^- ratio is a robust and reliable metric for the balance between PC and PDH.

We observed dramatic differences (×39) of [1-^{13}C]aspartate/[^{13}C]HCO_3^- between the fasted and the fed rats (Fig.3C). The observation is similar to a recent rat study using NMR that presented a significant difference between the PC/PDH ratio in fasted and fed conditions with a more than 50-fold difference(8). Another previous study with [1-^{14}C]pyruvate tracing and enzymatic assay in rat hepatocytes showed a similar trend of PC/PDH ratio(27).

One of the primary limitations of this study was the relatively small chemical shift dispersion at 3T. Therefore, to image spatial distribution of aspartate, a spectroscopic imaging approach that allows high spectral resolution with high signal sensitivity will be necessary. For instance, large flip angle excitations with narrow-band spectroscopic readouts around 160 ppm and 175 ppm in an interleaved fashion can be considered(28). Because of limited dispersion and additional polarization losses during the backward scrambling, we were unable to detect other PC-specific metabolites such as malate and OAA as described in a previous study at 9.4T(9). Another limitation of the study is the usage of transmit/receive ^{13}C surface coil and non-selective RF excitation. In addition to the convenient localization of the liver without utilizing slice-selective or phase-encoding gradients and the high signal sensitivity, we utilized a non-selective RF pulse for improved metabolite quantification in absorption mode by shortening the pulse width, and thus, minimizing the linear phase across the spectra. However, the method is exposed to potential signal contamination of non-hepatic tissues although probably not significantly, considering the liver volume and the proximity of the coil to the liver. The inhomogeneous B_1^+ profile also results in inconsistent RF excitation over the liver region, leading to suboptimal corrections of RF loss in the kinetic analysis. Moreover, as the SPINlab polarizer was designed for large human dosages, solid-state polarization buildup of the small lactate samples that we used in the study could

not be monitored, and therefore, the variability of the polarization level between samples was not corrected by polarization level. To counter that, we put in same volume of [1-^{13}C]-L-lactate from the same stock and matched the polarization time by curating the injection time.

Conclusion

Feasibility of simultaneously assessing hepatic PC and PDH activities using hyperpolarized [1-^{13}C]-L-lactate was demonstrated by detecting aspartate and HCO_3^- production *in vivo*.

Supplementary Material

Refer to Web version on PubMed Central for supplementary material.

Acknowledgements

Texas Institute for Brain Injury and Repair; The Mobility Foundation; National Institutes of Health of the United States (S10 OD018468, S10 RR029119, P41 EB015908); The Welch Foundation (I-2009-20190330); UT Dallas Collaborative Biomedical Research Award (UTD 1907789).

References

1. Utter MF, Keech DB. Formation of oxaloacetate from pyruvate and carbon dioxide. J Biol Chem. 1960;235:Pc17–8. [PubMed: 13840551]
2. Jitrapakdee S, Vidal-Puig A, Wallace JC. Anaplerotic roles of pyruvate carboxylase in mammalian tissues. Cell Mol Life Sci. 2006;63(7–8):843–54. [PubMed: 16505973]
3. Lao-On U, Attwood PV, Jitrapakdee S. Roles of pyruvate carboxylase in human diseases: from diabetes to cancers and infection. J Mol Med (Berl). 2018;96(3–4):237–47. [PubMed: 29362846]
4. Ardenkjaer-Larsen JH, Fridlund B, Gram A, Hansson G, Hansson L, Lerche MH, et al. Increase in signal-to-noise ratio of > 10,000 times in liquid-state NMR. Proc Natl Acad Sci U S A. 2003;100(18):10158–63. [PubMed: 12930897]
5. Golman K, Zandt RI, Lerche M, Pehrson R, Ardenkjaer-Larsen JH. Metabolic imaging by hyperpolarized 13C magnetic resonance imaging for in vivo tumor diagnosis. Cancer Res. 2006;66(22):10855–60. [PubMed: 17108122]
6. Merritt ME, Harrison C, Sherry AD, Malloy CR, Burgess SC. Flux through hepatic pyruvate carboxylase and phosphoenolpyruvate carboxykinase detected by hyperpolarized 13C magnetic resonance. Proc Natl Acad Sci U S A. 2011;108(47):19084–9. [PubMed: 22065779]
7. Merritt ME, Harrison C, Storey C, Jeffrey FM, Sherry AD, Malloy CR. Hyperpolarized 13C allows a direct measure of flux through a single enzyme-catalyzed step by NMR. Proc Natl Acad Sci U S A. 2007;104(50):19773–7. [PubMed: 18056642]
8. Jin ES, Moreno KX, Wang JX, Fidelino L, Merritt ME, Sherry AD, et al. Metabolism of hyperpolarized [1-(13)C]pyruvate through alternate pathways in rat liver. NMR Biomed. 2016;29(4):466–74. [PubMed: 26836042]
9. Lee P, Leong W, Tan T, Lim M, Han W, Radda GK. In vivo hyperpolarized carbon-13 magnetic resonance spectroscopy reveals increased pyruvate carboxylase flux in an insulin-resistant mouse model. Hepatology. 2013;57(2):515–24. [PubMed: 22911492]
10. Stubbs M, Veech RL, Krebs HA. Control of the redox state of the nicotinamide-adenine dinucleotide couple in rat liver cytoplasm. Biochem J. 1972;126(1):59–65. [PubMed: 4342386]
11. Veech RL. The metabolism of lactate. NMR Biomed. 1991;4(2):53–8. [PubMed: 1859786]
12. Veech RL, Raijman L, Krebs HA. Equilibrium relations between the cytoplasmic adenine nucleotide system and nicotinamide-adenine nucleotide system in rat liver. Biochem J. 1970;117(3):499–503. [PubMed: 4315932]

13. Hoffer LJ. Cori cycle contribution to plasma glucose appearance in man. JPEN J Parenter Enteral Nutr. 1990;14(6):646–8. [PubMed: 2273534]

14. Wang D, Yang H, De Braganca KC, Lu J, Yu Shih L, Briones P, et al. The molecular basis of pyruvate carboxylase deficiency: mosaicism correlates with prolonged survival. Mol Genet Metab. 2008;95(1–2):31–8. [PubMed: 18676167]

15. Mayer D, Yen YF, Josan S, Park JM, Pfefferbaum A, Hurd RE, et al. Application of hyperpolarized [1-(1)(3)C]lactate for the in vivo investigation of cardiac metabolism. NMR Biomed. 2012;25(10):1119–24. [PubMed: 22278751]

16. Park JM, Josan S, Mayer D, Hurd RE, Chung Y, Bendahan D, et al. Hyperpolarized 13C NMR observation of lactate kinetics in skeletal muscle. J Exp Biol. 2015;218(Pt 20):3308–18. [PubMed: 26347554]

17. Kennedy BWC, Kettunen MI, Hu D-E, Brindle KM. Probing lactate dehydrogenase activity in tumors by measuring hydrogen/deuterium exchange in hyperpolarized l-[1-(13)C,U-(2)H]lactate. J Am Chem Soc. 2012;134(10):4969–77. [PubMed: 22316419]

18. Bastiaansen JA, Cheng T, Mishkovsky M, Duarte JM, Comment A, Gruetter R. In vivo enzymatic activity of acetylCoA synthetase in skeletal muscle revealed by (13)C turnover from hyperpolarized [1-(13)C]acetate to [1-(13)C]acetylcarnitine. Biochim Biophys Acta. 2013;1830(8):4171–8. [PubMed: 23545238]

19. Takado Y, Cheng T, Bastiaansen JAM, Yoshihara HAI, Lanz B, Mishkovsky M, et al. Hyperpolarized (13)C Magnetic Resonance Spectroscopy Reveals the Rate-Limiting Role of the Blood-Brain Barrier in the Cerebral Uptake and Metabolism of l-Lactate in Vivo. ACS Chem Neurosci. 2018;9(11):2554–62. [PubMed: 29771492]

20. Chen AP, Lau JY, Alvares RD, Cunningham CH. Using [1-(13) C]lactic acid for hyperpolarized (13) C MR cardiac studies. Magnetic resonance in medicine. 2015;73(6):2087–93. [PubMed: 25046652]

21. van Heeswijk RB, Laus S, Morgenthaler FD, Gruetter R. Relaxivity of Gd-based contrast agents on X nuclei with long intrinsic relaxation times in aqueous solutions. Magn Reson Imaging. 2007;25(6):821–5. [PubMed: 17448617]

22. Jeoung NH, Harris RA. Role of pyruvate dehydrogenase kinase 4 in regulation of blood glucose levels. Korean Diabetes J. 2010;34(5):274–83. [PubMed: 21076574]

23. Exton JH, Corbin JG, Harper SC. Control of gluconeogenesis in liver. V. Effects of fasting, diabetes, and glucagon on lactate and endogenous metabolism in the perfused rat liver. J Biol Chem. 1972;247(16):4996–5003. [PubMed: 5061605]

24. Atherton HJ, Dodd MS, Heather LC, Schroeder MA, Griffin JL, Radda GK, et al. Role of pyruvate dehydrogenase inhibition in the development of hypertrophy in the hyperthyroid rat heart: a combined magnetic resonance imaging and hyperpolarized magnetic resonance spectroscopy study. Circulation. 2011;123(22):2552–61. [PubMed: 21606392]

25. von Morze C, Chang GY, Larson PE, Shang H, Allu PK, Bok RA, et al. Detection of localized changes in the metabolism of hyperpolarized gluconeogenic precursors (13) C-lactate and (13) C-pyruvate in kidney and liver. Magn Reson Med. 2017;77(4):1429–37. [PubMed: 27098724]

26. Keshari KR, Kurhanewicz J, Macdonald JM, Wilson DM. Generating contrast in hyperpolarized 13C MRI using ligand-receptor interactions. Analyst. 2012;137(15):3427–9. [PubMed: 22655289]

27. Agius L, Alberti KG. Regulation of flux through pyruvate dehydrogenase and pyruvate carboxylase in rat hepatocytes. Effects of fatty acids and glucagon. Eur J Biochem. 1985;152(3):699–707. [PubMed: 3932072]

28. Josan S, Hurd R, Park JM, Yen YF, Watkins R, Pfefferbaum A, et al. Dynamic metabolic imaging of hyperpolarized [2-(13) C]pyruvate using spiral chemical shift imaging with alternating spectral band excitation. Magn Reson Med. 2014;71(6):2051–8. [PubMed: 23878057]

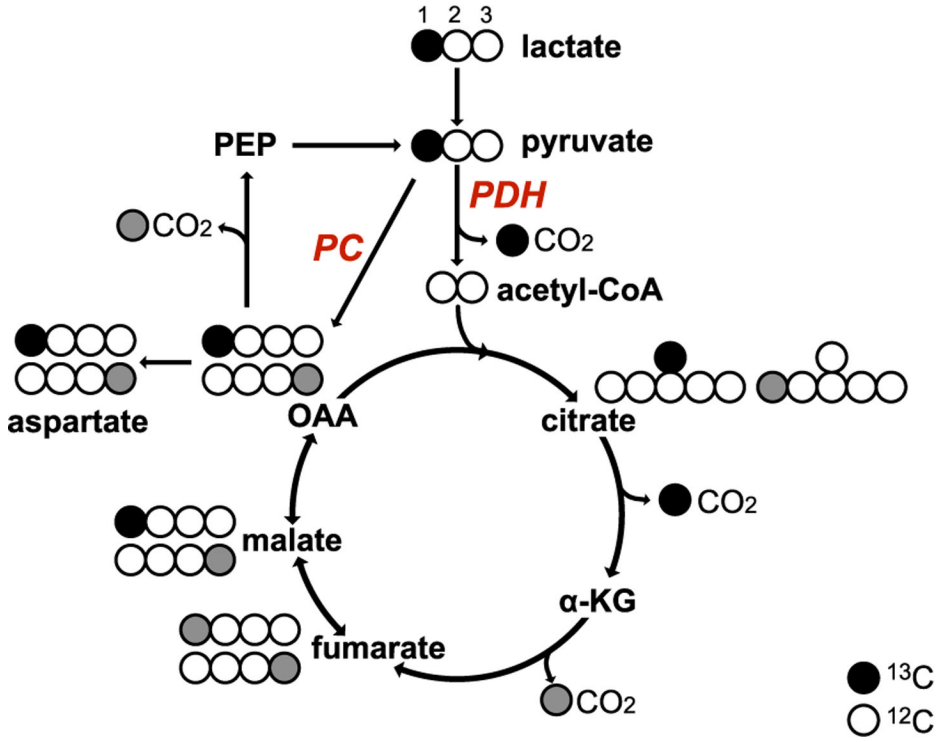

Figure 1. Flux of [1-^{13}C]-L-lactate.

[1-^{13}C]-L-lactate (black circle: ^{13}C, white circle: ^{12}C) is converted to [1-^{13}C]pyruvate, which is either converted into [1-^{13}C]oxaloacetate (OAA) through PC, or into acetyl-CoA and $^{13}CO_2$ through PDH. [1-^{13}C]OAA is converted into [6-^{13}C]citrate and the labeled carbon (^{13}C) is released as CO_2 when converted to α-ketoglutarate (α-KG). The exchange between malate and fumarate leads to the [4-^{13}C]malate and [4-^{13}C]fumarate (gray circle) and subsequent labeling at [4-^{13}C]OAA and subsequent [1-^{13}C]citrate.

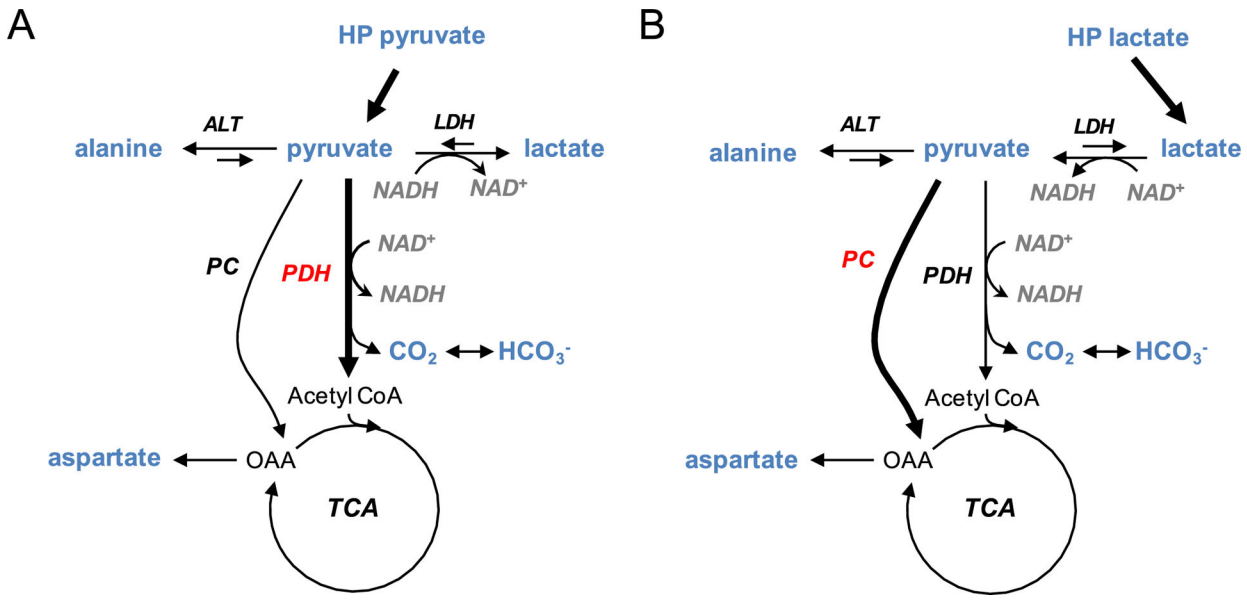

Figure 2.

Effects of a bolus injection of hyperpolarized (A) [1-^{13}C]pyruvate and (B) [1-^{13}C]-L-lactate on the cellular redox and the PDH/PC balance. Rapid conversion of pyruvate to lactate generates NAD^+, significantly altering cellular redox. Lactate has much less effect on redox.

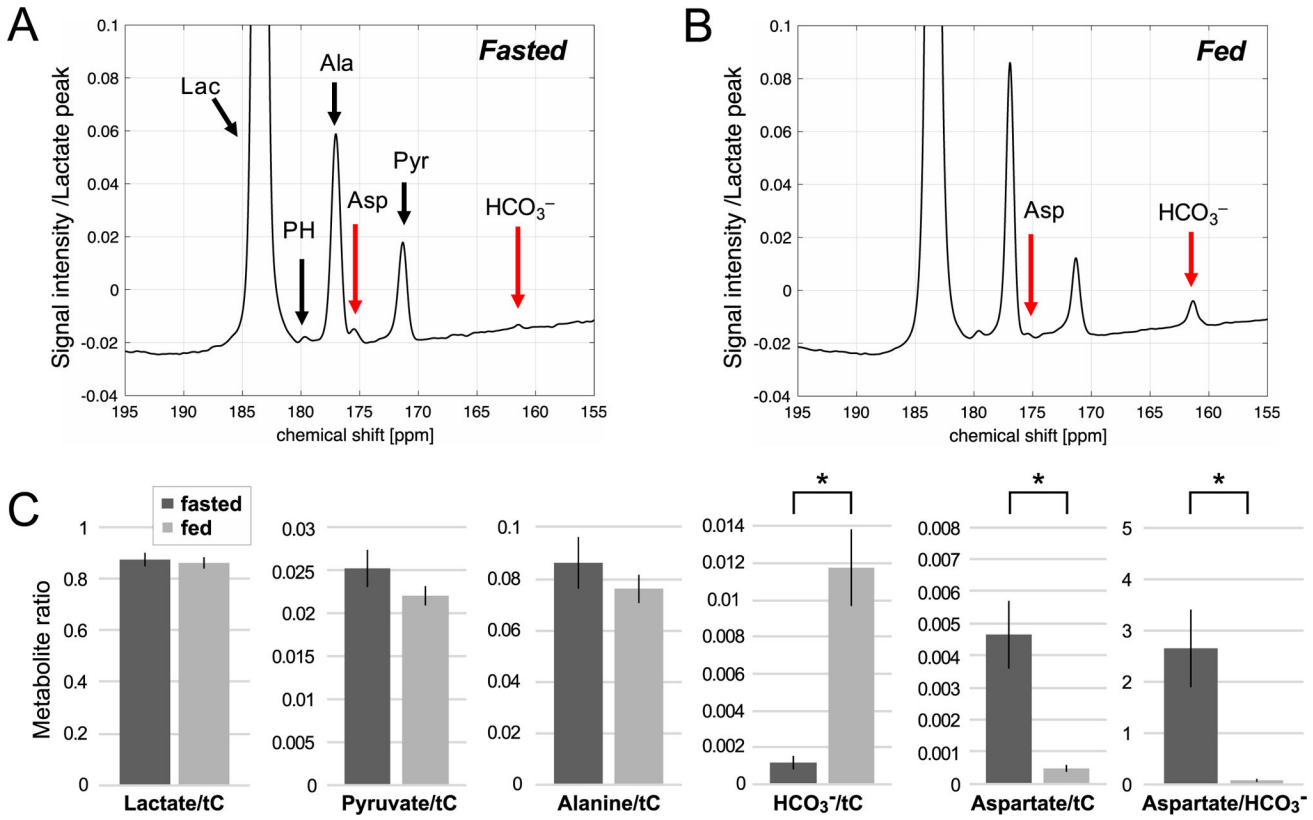

Figure 3.

Time-averaged spectra of 60-mM hyperpolarized [1-^{13}C]-L-lactate in the liver of (A) fasted and (B) fed rats. The spectrum is normalized to the maximum [1-^{13}C]lactate peak intensity. (C) Comparison of lactate signals and products, normalized by the total hyperpolarized carbon (tC) signals in the fasted and fed groups. * indicates statistical significance between the groups ($P < 0.01$). Lac: lactate, PH: pyruvate hydrate, Ala: alanine, Asp: aspartate, Pyr: pyruvate, HCO_3^-: bicarbonate.

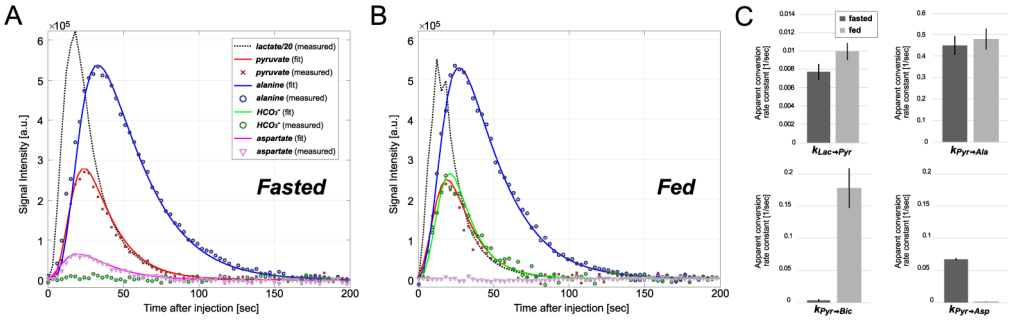

Figure 4.

Dynamic changes of lactate and products. Kinetics of pyruvate, alanine, bicarbonate (HCO_3^-), and aspartate (solid lines) were fitted to the measured metabolite time curves (scatter plots) using a multi-site exchange model in (A) fasted and (B) fed rat liver. (C) Comparison of apparent conversion rate constants between fasted and fed cohorts. Lac: lactate, Pyr: pyruvate, Ala: alanine, Asp: aspartate.

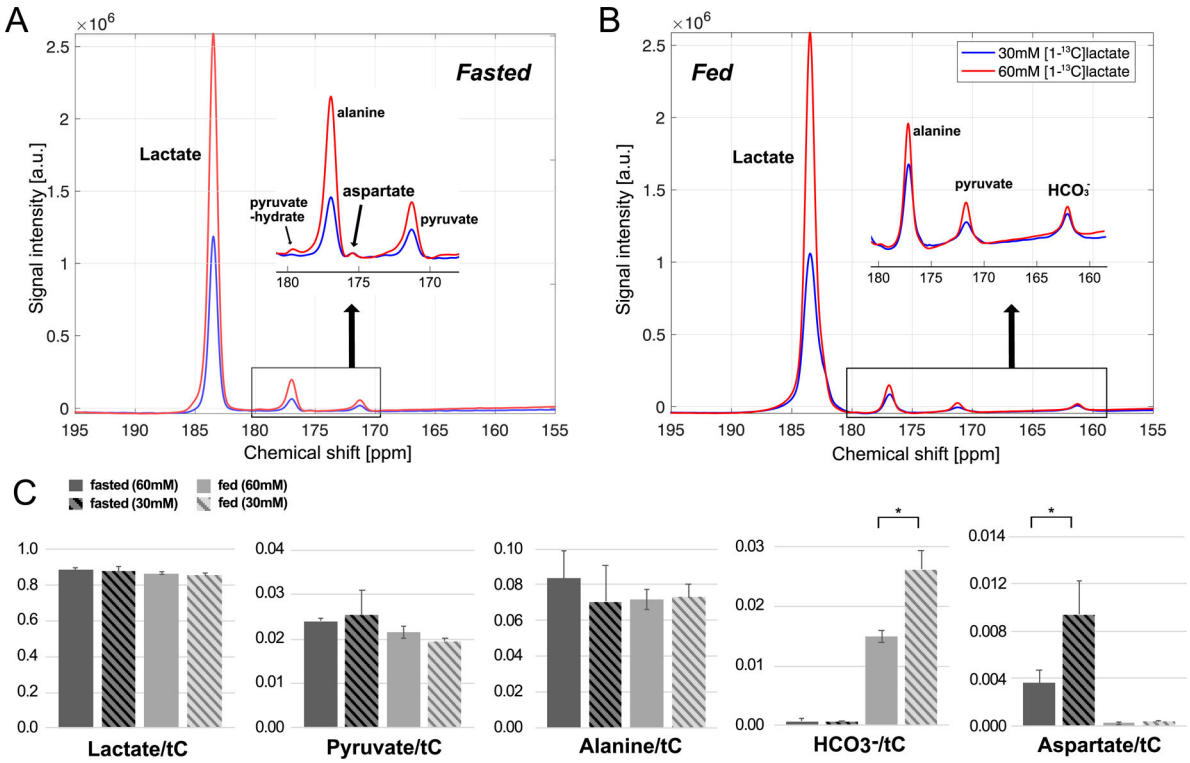

Figure 5.

Effect of different doses of [1-^{13}C]-L-lactate on [^{13}C]HCO_3^- and [1-^{13}C]aspartate production from a rat liver in (A) fasted and (B) fed nutritional states. Red spectra were acquired after a bolus injection of 60-mM hyperpolarized [1-^{13}C]lactate, and blue spectra were acquired with 30-mM [1-^{13}C]lactate. (C) Comparison of apparent conversion rate constants between 30-mM and 60-mM lactate in fasted and fed cohorts. Lac: lactate, Pyr: pyruvate, Ala: alanine, HCO_3^-: bicarbonate, Asp: aspartate.